Investigating grinding mechanisms and scaling criteria in a ball mill by dimensional analysis

Martin Giraud, Cendrine Gatumel, Stéphane Vaudez, Jeremy Nos, Thierry Gervais, Guillaume Bernard-Granger, Henri Berthiaux

Investigating grinding mechanisms and scaling criteria in a ball mill by dimensional analysis

Martin Giraud [a,b], Cendrine Gatumel [a], Stéphane Vaudez [b], Jeremy Nos [c], Thierry Gervais [d], Guillaume Bernard-Granger [b,*], Henri Berthiaux [a]

[a] Laboratoire RAPSODEE, UMR CNRS 5302, IMT Mines Albi, Campus Jarlard, 81013 Albi Cedex 09, France
[b] CEA, DES, ISEC, DMRC, Université Montpellier, 30200 Marcoule, France
[c] Orano, 125 avenue de Paris, 92320 Châtillon, France
[d] Orano Melox, Les Tourettes, D138A, 30200 Chusclan, France

A B S T R A C T

A dimensional analysis of the ball mill process is carried out through the Buckingham-Pi method. The dimensionless quantities identified are discussed and used in order to suggest scaling criteria for ball mills. The flowability and the particle size distribution of an alumina powder ground in laboratory ball mills of various dimensions are compared in order to discuss the influence and the relevance of each dimensionless numbers. Some geometrical, kinetics and dynamic similitudes are highlighted both theoretically and experimentally. In particular, the conservation of the Froude number and the fragmentation number lead to relevant scaling criteria for mills of 1, 2 and 7 L inner volumes. The importance of the ratio between the pebble size and the vessel diameter is also discussed. Finally, the preponderance of the fragmentation number over the number of revolutions of the vessel is interpreted in terms of particle fragmentation mechanisms.

Keywords:
Powder grinding - ball mill
Scale-up
Rheology
Dimensional analysis

1. Introduction

Ball mills are one of the most common industrial equipments for reducing the size of particulate systems in various fields such as cement industry, minerals or nuclear fuel production [1]. In such equipment, the powder is ground due to the movement of the grinding media, also called pebbles, within a rotating vessel. Grinding powders in a ball mill is a complex operation in which many parameters, such as geometrical factors [2], filling ratios [3], powder properties [4] or the energy transferred to the vessel [5] can influence the characteristics of the resulting powder. The effect of each parameter on the resulting ground powder is usually investigated experimentally in small vessels, designed at a laboratory scale before adjusting the parameters on the industrial equipment. However, the variety of the parameters involved leads to many difficulties for identifying the scale-up criteria that allows getting similar results in vessels of various sizes [6]. Considering the number of variables, dimensional analysis is a natural way to address this issue by regrouping all the variables in a limited number of dimensionless quantities.

Three mechanisms are classically identified as responsible for the particle fragmentation in a ball mill: compression due to the weight of the pebbles bed, shearing at the contact points between the pebbles or against the wall of the mill and impact caused by the ballistic effect due to the ejection of some pebbles from the bed. Those three mechanisms are competing and the predominance of a given fragmentation mode over the others depends on particles properties and also on the motion of the pebbles within the rotating vessel [7]. A typical classification, suggested by Mellmann, includes three main motion regimes of the pebbles in such an equipment: slipping, cascading and cataracting, which are themselves divided into seven sub-regimes [8]. The slipping motion is characterized by a pebbles bed remaining at rest and slipping periodically or continuously from the wall of the vessel. This motion usually appears at very low rotational speeds and mostly involves particle fragmentation through shearing and compaction mechanisms. When the vessel's rotational speed increases, a continuous circulation of the pebbles takes place, which corresponds to a cascading motion. Here, the pebbles are falling at the surface of the pebbles bed while the bottom part of the bed is lifted upwards by the motion of the wall. The cascading regime can be divided itself in three sub-regimes: slumping, rolling and cascading that corresponds respectively to higher rotational speeds. In such

* Corresponding author.
E-mail address: guillaume.bernard-granger@cea.fr (G. Bernard-Granger).

Nomenclature

Notation	Parameter and usual units
a	Chamfer size mm
$Bo_{g,i}/Bo_{g,f}$	Granular Bond number of the powder before / after grinding -
D_0/D_i	Outer / inner diameter of the vessel mm
d_g	Diameter of a pebble mm
d_s	Sauter mean diameter of the powder μm
d_{50}	Median diameter of the powder μm
f_c	Powder filling ratio -
ff_c	Flow function coefficient of the powder -
$F_{IP,i}/F_{IP,j}$	Interparticle attractive forces before / after grinding N
Fr	Froude number -
g	Gravity acceleration m.s^{-2}
h_0	Height of the pebble bed mm
J	Pebbles filling ratio -
k	Number of elementary dimensions -
L	Length of the vessel mm
l_g	Length of a pebble mm
m_p	Mass of powder g
n	Number of physical parameters -
n_f	Fragmentation number -
N_g	Number of pebbles -
N_t	Number of revolutions of the vessel -
p	number of dimensionless quantities -
$\wp_i/\wp_f$	Vector of particle properties before / after grinding various
t	Grinding time min
U	Powder level -
V	Inner volume of the vessel L
$V_{\text{pebble}}; V_{\text{powder}}$	Volume of pebbles /powder within the vessel mL
v_g	Velocity of a pebble at the surface of the bed cm.s^{-1}
v_w	Wall velocity of the vessel cm.s^{-1}
W_p	Particle's weight N
β	Intermediate variable -
δ	Pebble to vessel size ratio -
ε_g	Porosity of the pebbles bed -
$\lambda; \lambda_g$	Vessel / pebble geometric ratio -
μ_w	Wall friction coefficient -
ν	Velocity ratio -
π_i	dimensionless quantity$i \in [0, p]$ -
$\rho_g; \rho_p$	Density of the pebble / powder g.cm^{-3}
ρ_s	True density of the powder g.cm^{-3}
σ_0	Particle fragmentation tensile stress threshold g.m.s^{-2}
τ_0	Characteristic time for particle fragmentation s
ϕ	Slope angle of the pebble bed
ω	Angular velocity of the vessel rad.s^{-1}
Ω	Rotational speed of the vessel rpm

regimes, the particle fragmentation is mostly governed by impact and shearing phenomena as consequences of pebbles motion. Finally, the cataracting motion regime corresponds to the ejection of some individual pebbles from the surface of the bed that are projected in the free space of the vessel. According to Mellmann, the motion regime that takes place into the vessel depends mainly on the wall friction coefficient, the vessel filling ratio and the Froude number, Fr, being defined by equation (1) by the ratio between the centrifugal and gravitational forces acting on the pebbles located at the wall of the vessel.

$$Fr = \frac{D_i \omega^2}{2g} \tag{1}$$

where D_i is the inner vessel diameter, g is the gravity constant and ω is the angular velocity of the vessel, expressed in rad.s^{-1}.

The purpose of the ball milling process is to reduce the size of the particles constituting the powder. Since the powder is made of multiple particles, some mean or median diameters, such as the Sauter mean diameter, are commonly used to describe the overall particle size distribution. However, these average diameters usually fail to take into account the population of the fine particles that appears to be critical for the flow behavior of the whole powder, although it is a key parameter to control in a powder process plant. Indeed, recent studies highlighted the link between the macroscopic flowability of a given powder and its particle size distribution and showed that the fine particles, that may be generated by grinding, drastically decrease powder's flowability [9–11]. According to this study, the flow properties of a given powder can be considered as representative of the amount of fine particles generated by grinding. The properties of the ground powders, obtained by the ball milling process, can then be assessed directly by analyzing their flow behavior. Thus, the scale-up criteria investigated in this study should provide ground powders of similar flowability whatever the size of the vessel.

Dimensional analysis consists in regrouping all the physical variables that affect the final product properties, in a limited number of dimensionless groups [12,13]. The obtained dimensionless numbers lead to the definition of scaling criteria, which can be employed for designing mock-up processes at laboratory scales or deducing the behavior of a process at industrial scale from laboratory experiments [14]. In our case, the dimensional analysis of the ball milling process will be carried out in order to get a physically meaningful equation between the properties of the final product, like its flowability, and the geometrical and operational process parameters at any scale. This will help identifying the most relevant criteria that can be used for replicating similar grinding conditions at various scales. The establishment of such a process relation needs a prior knowledge of the influence of the most obvious operating conditions on the resulting powder. This means that a preliminary experimental investigation should be carried out as a guidance through the dimensional analysis.

Up to now, most of the scaling criteria identified for the ball mill process come from the investigation of the motion of granular media in rotating drum, without pebbles. Dimensional analysis has been extensively applied to describe the flow behavior of powders in rotating cylinders [15,16], providing scaling criteria usually based on the Froude number or on the vessel's wall velocity. The motion of granular materials within a rotating drum has also been investigated by analyzing the velocity profile of the particles. This can be achieved by filming the motion of the particles within the vessel [5] or using more advanced techniques, such as tracking the particles with fiber-optic probes [17]. Discrete element method (DEM) simulations of the particles flow in a rotating drum has also been carried out [18,19]. The main advantage of this latter approach is its ability to take into account more parameters in a wider range than those available in experimental studies. However, the investigations listed in this paragraph mainly focus on the motion of the powder only and do not take into account the interaction between the powder and the pebbles, which is responsible for particle fragmentation in a ball mill. In such equipment, it can be considered that the motion of the pebbles and powder bed is mostly driven by the pebbles, which are not expected to behave

the same way than microscopic powders in a rotating drum. To go further, embedding the grinding media in the dimensional analysis of the ball mill would be of great interest.

Accordingly, the aim of this paper is to identify which dimensionless numbers must be kept constant in order to reproduce the results obtained in a laboratory ball mill at the industrial scale. Such scaling criteria are provided by an exhaustive dimensional analysis applied to the ball mill. In particular, the motion of the pebbles within the rotating vessel will be investigated from video analysis and linked to the ground powder properties. The results will be tested experimentally by measuring the characteristics of powders ground in vessels of different volumes and under various grinding conditions. The ground powder properties are assessed from their rheological behavior. The main operational parameters investigated include equipment dimensions, filling ratios and parameters related to the vessel's motion.

The materials and the methods involved in this study will be presented in section 2. Then, a primary investigation, including a velocimetry analysis of the pebbles bed motion and the investigation of the most common operating parameters in a one-sized vessel will be presented in section 3. Based on these preliminary results, the dimensional analysis of the ball mill process will be described in section 4. Finally, the scaling criteria will be tested experimentally in vessels of three different sizes, as reported in section 5.

2. Materials and methods

2.1. Powders and characterization methods

2.1.1. Powder used

An alumina GE15 (Al_2O_3) powder, from Baikowski® (Poisy, France) was used for this investigation. Its particle size distribution in volume is represented on Fig. 1. The measurement was carried out by LASER diffraction in a Mastersizer 3000® (Malvern, Malvern, UK), equipped with a liquid water dispersion unit Hydro MV®. The measured particle diameters range from 0.9 to 110μm with a volume median diameter of $d_{50} = 33.9\mu m$ and a Sauter mean diameter of $d_s = 19.8\mu m$. SEM pictures of the particles constituting the alumina powder are shown before and after grinding on Fig. 2, for magnitudes of x100 and x800. Even before grinding, the particles exhibit an irregular and angular shape.

The scope of this study mainly focuses on the mill parameters, such as its dimensions, rotation speed, filling ratios and grinding time. Therefore, only one powder was used for the whole investigation so that it is always the same powder that is being ground. Thus, the particles properties such as their plasticity, hardness or brittleness are not considered in this study, although they could have a great influence on the fragmentation mechanisms.

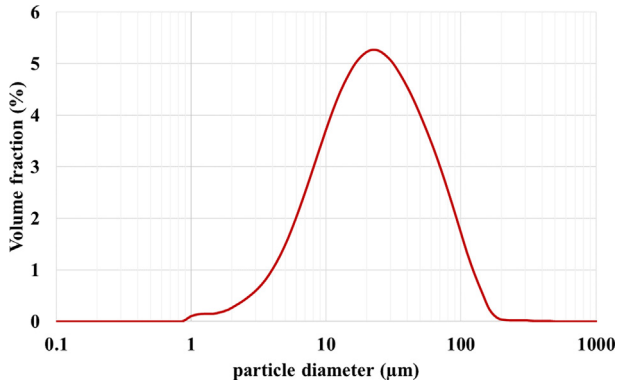

Fig. 1. Volume particle size distribution of the alumina GE15 powder, measured by LASER dispersion in wet mode.

2.1.2. Powder flowability measurements

The powder flowability was measured with a FT4® (Freeman, Tewkesbury, UK) powder rheometer. Shear tests were carried out in a 10 mL cylindrical cell made of borosilicate glass under a normal pre-consolidation stress of 9 kPa, following the Jenike standard procedure [20]. During the tests, a powder sample is introduced into the cell and sheared under normal consolidation stresses of 7, 6, 5, 4 and 3kPa successively. The minimal tangential stress needed to yield the powder sample under each normal stress is measured and the obtained data lead to the determination of the yield locus and the Mohr's circles equation parameters. Finally, several characteristics related to the flowability of the powder can be computed from geometrical considerations. More details concerning this technique can be found elsewhere in the literature [21,22]. In particular, the flow function coefficient ff_c is commonly employed to assess and rank the flow behavior of powders according to the classification given in Table 1.

2.2. Experimental device

The powder samples were ground in a ball mill which is a cylindrical vessel made of stainless steel that is filled with cylindrical steel pebbles. The cylindrical shape of the pebbles was chosen in order to match a specific industrial setup, although spherical pebbles are more common in the grinding processes. The powder was introduced within the vessel and the pebbles act as grinding media while the vessel is rotating horizontally around its longitudinal axis as shown in Fig. 3. The rotation of the vessel is controlled by a potentiometer graduated from 0 to 100 and the rotational speed was measured by a tachymeter DT-2236® (Lutron electronic, Taipei, Taiwan). No contamination of the ground powder by the pebbles and wall materials was observed, even for high rotation speeds. In this paper, we will use Ω to describe the rotational speed of the vessel, expressed in revolutions per minute (rpm), while ω represents the corresponding angular velocity, expressed in radians per second ($\omega = \frac{2\pi}{60}\Omega$). Both vessel lids are made of transparent poly(methyl methacrylate) (PMMA) allowing the capture of the pebbles motion during the rotation of the vessel. More details about this technique are provided in section 2.3.

Three different vessels of 1, 2 and 7 L (typically represented on Fig. 4) were used for the experimental investigation of the ball mill scaling. The 1 and 2 L vessels were designed with a chamfer inside the cylinder at both extremities (see Fig. 4) in order to avoid the retention of powder in the angles and to be able to fix both PMMA lids with screws. However, the 7 L vessel could not be made with chamfers and was designed with stainless steel lids instead of transparent PMMA ones. The inner and outer diameters D_i and D_o, the length L and the chamfer size a of those three vessels are given in Table 2. The vessels were specially designed to keep the geometric ratio $\lambda = D_i/L$ constant, the reason for this coming from the dimensional analysis that will be presented in section 4.1. Finally, two sizes of steel cylindrical pebbles were available for this study: 8x8 mm and 15x15 mm.

2.3. Measurement of the pebbles velocity profile

The motion of the pebbles inside the vessel was investigated by tracking their position along the surface of the pebbles bed from videos acquired when the vessel was rotating. Several videos were taken with various amounts of pebbles and under various rotational speeds. This was carried out for the 1 L and 2 L vessels only because the 7 L vessel could not be manufactured with transparent

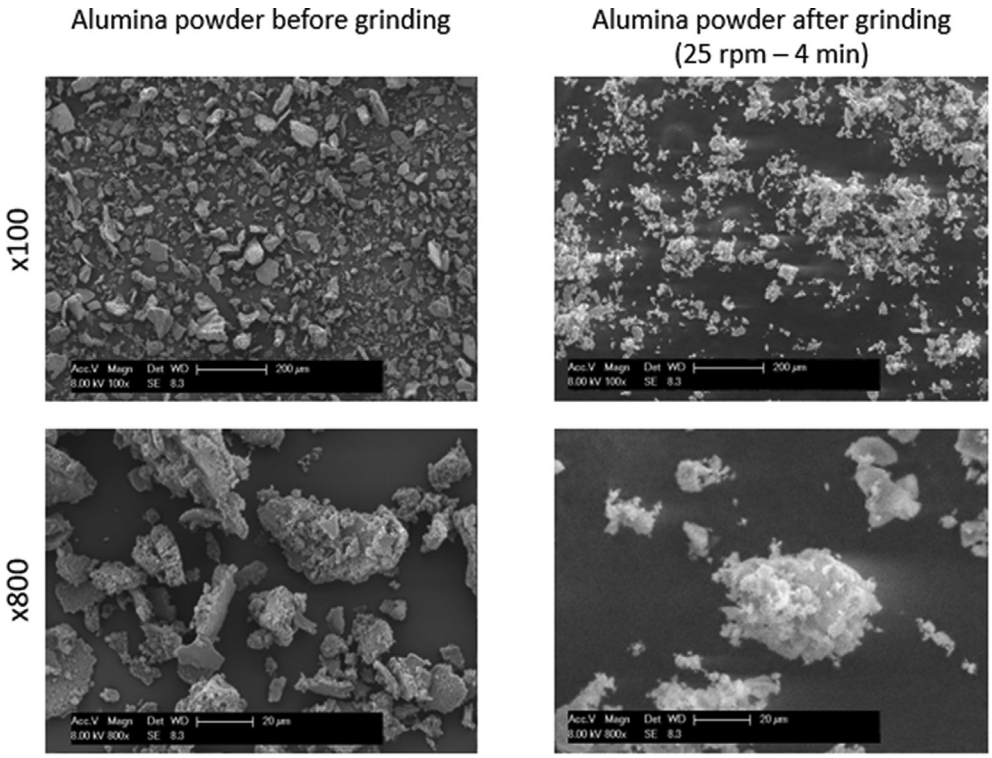

Fig. 2. SEM pictures (x100 and x800 magnitude) of the alumina powder, before (left) and after grinding in the 1 L vessel at 25 rpm for 10 min (right).

Table 1
Classification of the flowability of a given powder measured by shear testing according to its.

Flow index value	Flowability
$ff_c < 1$	Not flowing
$1 < ff_c < 2$	Very poor
$2 < ff_c < 4$	Poor
$4 < ff_c < 10$	Easy
$ff_c > 10$	Free flowing

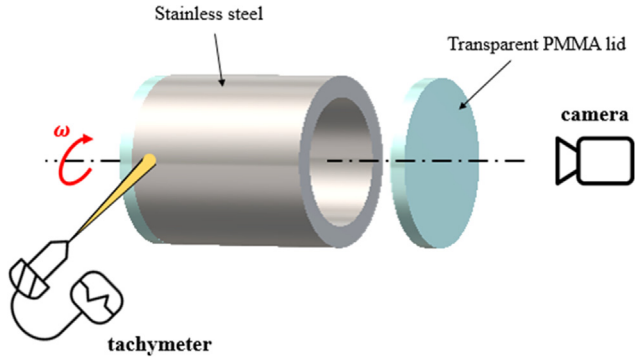

Fig. 3. Schematic representation of the ball milling setup.

lids. No powder was introduced in the vessels while recording the videos in order to be able to locate the pebbles more easily. The camera, recording at 240 frames per second for about ten seconds after reaching the permanent regime inside the vessel, was positioned in the longitudinal axis of the vessel, as shown in Fig. 3. After separating the videos frame by frame, the position of some pebbles that were chosen arbitrarily were tracked and recorded every two frames ($4ms$) using the ImageJ® (NIH, Bethesda, USA) software. An example of snapshot obtained is given in Fig. 5. The size conversion from pixel to centimeters was achieved by adjusting the scale from the vessel diameter, which is known precisely. The velocity of the pebbles was then computed by calculating the distance travelled between consecutive snapshots.

One of the biggest source of incertitude related to this approach arose from the cylindrical shape of the pebbles, as their center of gravity is hard to locate when they are spinning. This point is even more critical considering the fact that the size of a pebble represents between 5 and 12% of the inner diameter of the vessel, depending on the configuration (vessel and pebbles chosen). It should also be noted that only the pebbles located at the lids vicinity are visualized by the camera and that their displacement along the longitudinal axis was not taken into account.

3. Primary investigation

In this investigation, the pebbles motion corresponds mainly to a cascading regime, meaning that the particle fragmentation occurs by shearing and impact mechanisms induced by the interactions of the pebbles with each other and with the vessel walls. Thus, in order to guide us through the dimensional analysis of the ball mill process, a primary investigation concerning the pebbles motion inside the vessel must be carried out. This will serve to further investigate the influence of the most common parameters on the flowability of the ground powder.

3.1. Investigating the pebbles motion within the vessel

The velocity of the pebbles inside the 1 L and 2 L vessels has been investigated, following the methodology described in section 2.3, for various rotational speeds: $\Omega = 20$, 30, 40 and 50 rpm. For each configuration, between five and ten pebbles were tracked in order to get their velocity profiles. Among the pebbles at the surface of the powder bed, the ones that were less affected by

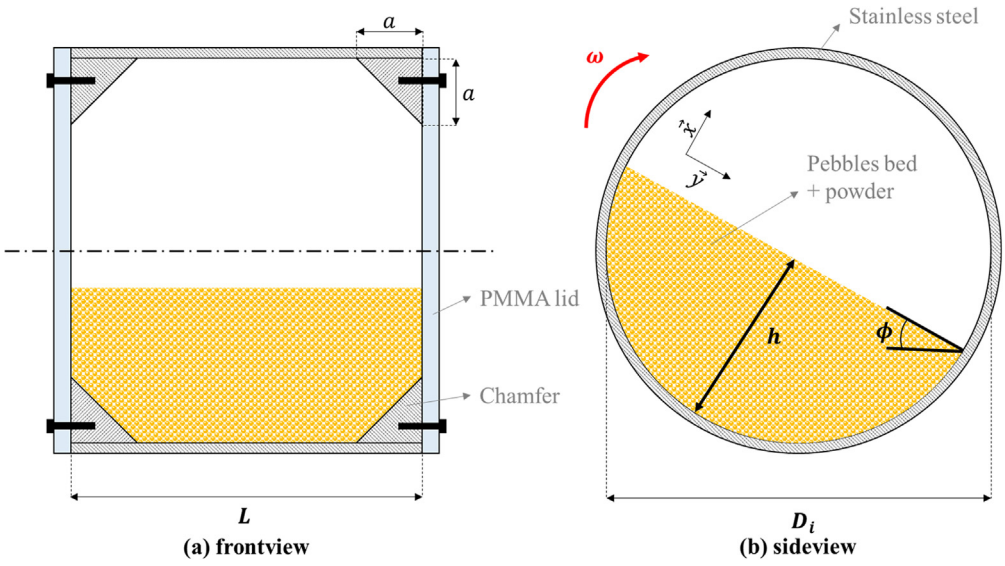

Fig. 4. Schematic representation of the ball mill filled with pebbles.

Table 2
Dimensions of the different vessels, represented in Fig. 4, used in this study.

Dimension	Notation	1 L vessel	2 L vessel	7 L vessel
Outer diameter (mm)	D_o	126	155	224
Inner diameter (mm)	D_i	116	145	214
Length (mm)	L	106	131	195
Chamfer size (mm)	a	20	20	0
Size ratio	$\lambda = D_i/L$	1.1	1.1	1.1

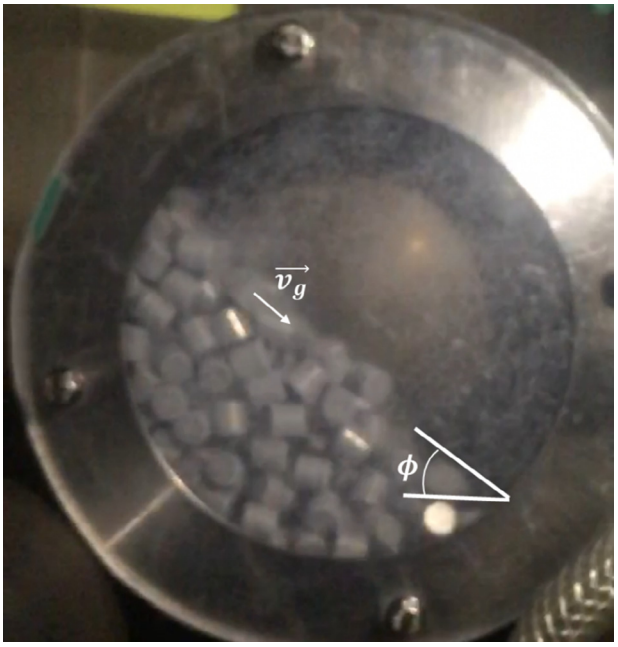

Fig. 5. Example of snapshot obtained for the 2 L vessel rotating at 20 rpm, filled with 8x8 mm pebbles at J = 0.3 and without powder.

collisions with other pebbles were arbitrarily chosen in order to measure their maximal fall speed. For each case, the mean velocity profiles of the selected pebbles could be modeled by a second order polynomial interpolation, an example being given on Fig. 6. The maximal speed of a falling pebble is assumed to correspond to the summit of the parabola as shown on Fig. 6. This critical velocity, denoted as v_g^{max}, represents the maximal speed that may be reached by a pebble falling along the surface of the bed for a given vessel rotational speed. The dimensionless velocity ratio, υ, representing the ratio between the velocity of the pebbles at the surface of the bed and the linear velocity of the vessel, can thus be approximated by equation (2).

$$\upsilon \approx \frac{v_g^{max}}{v_w} \tag{2}$$

where v_w is the vessel's wall linear velocity, which is directly linked to its rotational speed according to equation (3).

$$v_w = \frac{D_i}{2}\omega \tag{3}$$

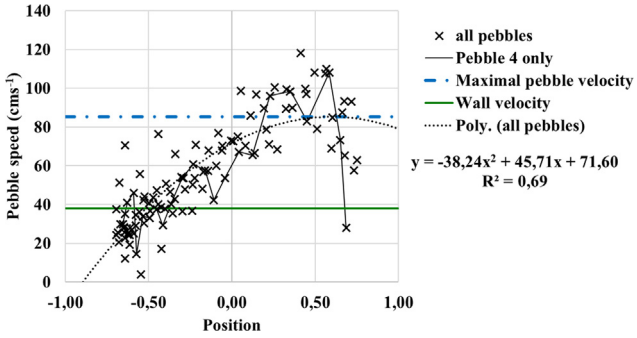

Fig. 6. Velocity profile of the pebbles at the surface of the pebbles bed in the 2 L vessel, rotating at 50 rpm. The velocity of a given pebble (pebble 4) is marked with the continuous dark line, the dotted curve represents the polynomial interpolation of the fall speed, the dotted straight line corresponds to the maximal velocity of the pebbles $v_{p,max}$ and the continuous straight line corresponds to the wall linear velocity v_w.

The evolution of the velocity ratio, v, according to the Froude number of the vessel, Fr, for the 1 and 2 L vessels is plotted on Fig. 7. Firstly, it has to be outlined that the correlation between those two non-dimensional parameters does not depend on the size of the vessel. It also appears on Fig. 7 that the velocity ratio decreases linearly with the Froude number up to $Fr = 0.13$ and becomes constant beyond this value, suggesting the existence of two different pebbles motion regimes within the vessel:

- for$Fr \geq 0.13$, the pebbles velocity is strictly proportional to the vessel wall velocity, suggesting that the motion of a given pebble is mostly due to the rotation of the vessel itself, which is typical of the cascading or cataracting regimes [8],
- For $Fr \leq 0.13$, the pebbles motion does not seem to be fully driven by the vessel motion but also depends on the collision events with other pebbles, which better fits with the rolling regime.

Such observations suggest that the transition between the rolling and cascading regimes corresponds to $Fr_{rol-cas} = 0.13$, which is consistent with the pebbles motion captured from the videos recorded. In a rolling regime, a free surface rolling flow of pebbles is taking place during the rotation of the vessel. The particles fragmentation are then more likely to occur continuously all along the surface of the pebbles bed by small collision and friction events between the pebbles. In cascading regimes, pebbles are ejected periodically from the free surface of the bed, then, a larger amount of fragmentation events may occur at the bottom of the pebbles bed, at the impact point of the falling pebbles. However, the preponderance of the fragmentation by impact and shearing mechanisms also depends on the nature and the size of the particles. An impact mechanism is more effective for larger particles, that have a typical diameter comprised in a range of $50\mu m$ to $5mm$ [7]. It should also be noted that a large number of small collisions between pebbles continues to occur in the cascade regime [23], which means that the particles are still susceptible to break under a shearing mechanism in such motion regime.

From the same recorded videos, the average slope angle of the pebbles bed, denoted as ϕ, is also computable by measuring the angle of the slope defined by the highest and the lowest pebbles in the vessel every $0.5s$ and by taking the average value. In order to simplify the investigation, the average value of the slope angle was taken as a characteristic parameter of the pebbles bed rotational regime. However, some recent results suggest that considering the ratio between the maximum slope angle and the average slope angle should be even more relevant [18]. The evolution of ϕ according to the Froude number is given in Fig. 8. The incertitude intervals correspond to the standard deviation, which is quite high since the slope angle seems to be oscillating. It appears that the average slope angle increases with the Froude number at the same rate whatever the size of the vessel.

3.2. Process parameters

Several grinding tests have been carried out with the alumina powder, in the 1 L vessel and for various grinding conditions. The obtained ground powders have been compared in terms of flowability in order to evaluate the influence of the most common grinding parameters. The parameters considered in this section are split into two distinct categories. First, the parameters related to the energy provided to the vessel, investigated in section 3.2.1, that include the vessel's rotational speed and the grinding time. Second, the filling parameters, investigated in section 3.2.2, corresponding to the powder and to the pebbles filling ratios.

3.2.1. Parameters linked to the energy provided to the vessel

The movement of the mill is fully defined by its rotational speed around the longitudinal axis of the vessel. Obviously, the influence of the rotational speed, Ω, on the properties of a ground powder cannot be investigated without taking into account the grinding time t. The hatched bars on Fig. 9 show the flow function coefficient obtained after grinding the powders for 4 min at 25, 36 and 50 rpm. Such rotational speeds all correspond to a similar rolling / cascading regime as described previously in section 3.1. The results on Fig. 9 show that the flow function coefficient becomes smaller when the vessel is rotating faster, meaning that the ground powder flowability decreases when Ω increases. The decrease of flowability observed after grinding tests can be explained by the particle size reduction that occurs during the ball milling process. Indeed, previous investigations have shown that the particle size was the most important parameter governing the flow behavior of a powder bed [9]. In particular, the flowability of a given powder appears to decrease drastically when the amount of small particles, under $10\mu m$ in diameter, increases. Thus, the flow function coefficient can be used as an indicator of the efficiency for a given grinding test: a small ff_c indicates a significant amount of fine particles, corresponding to an intensively ground powder. One can notice that the powder flowability may also be strongly influenced by the particle shape, which is expected to vary during the grinding process due to their fragmentation. However, it should be noted that in our case the grinding operation does not have a significant effect on the particle shape since they already are irregular and

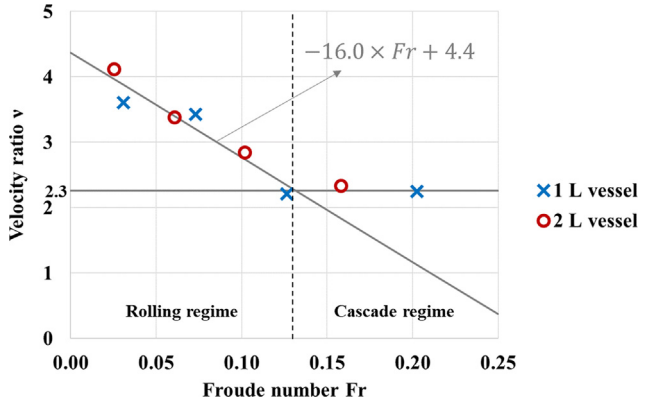

Fig. 7. Velocity ratio v (pebble/wall) as a function of the Froude number Fr in the 1 L (crosses) and 2 L (circles) vessels. The velocity ratio seems to be inversely proportional to the Froude number before $Fr = 0.13$ and constant after.

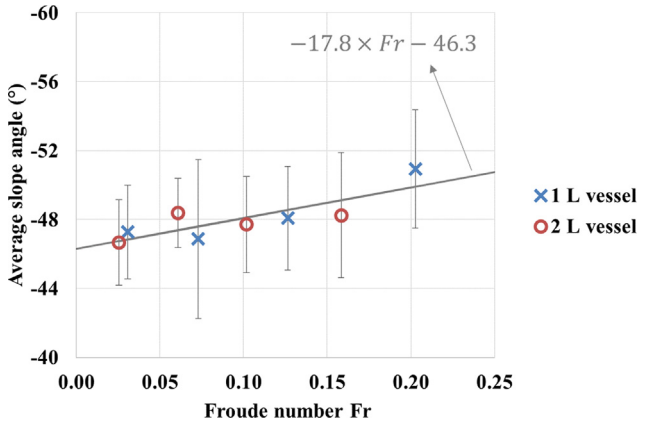

Fig. 8. Average slope angle of the pebble bed ϕ inside the 1 L (crosses) and 2 L (circles) vessels, as a function of the Froude number Fr.

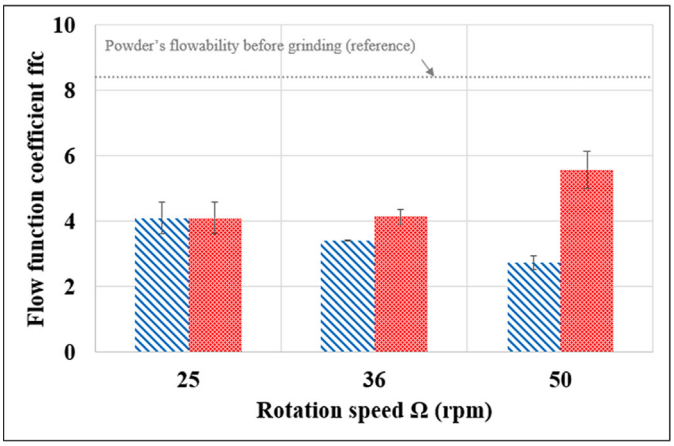

Ω (rpm)	25	36	50
	Hatched bars (left)		
t (min)	4	4	4
N_t (-)	100	144	200
	Dotted bars (right)		
t (min)	4	3	2
N_t (-)	100	100	100

: $t = 4\ min$ constant

: $N_t = 100$ constant

Fig. 9. Evolution of the flow function coefficient of ground powders according to the rotational speed of the vessel Ω at constant grinding time t (hatched bars, left) and constant number of revolutions N_t (dotted bars, right). All the grinding tests are performed in the same filling conditions with $J = 0.3$ and $U = 1.00$.

angular before grinding. Indeed, the SEM pictures shown on Fig. 2 show that the particles shape does not change drastically before and after grinding. This was already evidenced in a previous paper where the authors shown that the particle size is actually the most important parameter governing the flowability of this specific powder along the grinding process [24].

It is interesting to note that, in virtue of equation (4), increasing the rotational speed leads to a higher number of revolutions N_t of the vessel for a given amount of time.

$$N_t = \Omega \cdot t \tag{4}$$

The number of revolutions performed by the vessel in our examples are summarized in the table associated to Fig. 9. Another set of experiments were carried out by adjusting the grinding time according to the rotational speed in order to keep the number of revolutions constant at $N_t = 100$. The results are given by the dotted bars on Fig. 9. It appears that the powder samples ground at higher rotational speeds with a fixed number of revolution (dotted bars on Fig. 9) exhibit a slightly better flowability, meaning that they are less reduced in size. This is due to the smaller grinding time (given on the right of Fig. 9) required to achieve the fixed number of revolutions for higher rotational speeds.

A higher number of revolutions leads to a higher number of periodical impacts in the powder bed due to pebbles projected in cascade or cataract regimes and resulting in more particle fragmentation. However, the amount of such impacts does not have any influence on the shearing fragmentation mechanism, which occurs continuously within the pebbles bed. Thus, it can be assumed that the impact fragmentation mechanism is related to the number of revolutions of the vessel, N_t, while the shearing fragmentation mechanism is mostly governed by the grinding time, t. It is then of a great interest to clarify whether the ball milling process is governed by the grinding time or by the number of revolution in order to assess which fragmentation mechanism is the most critical. However, it should be noted that the fragmentation mechanisms depend on the rotational regime of the vessel and thus on the rotational speed imposed to the system. Therefore, Fig. 9 cannot provide much more information concerning the fragmentation mechanisms. Up to now, it remains unclear whether the flowability of the ground powder beds is governed by the grinding time or by the number of revolutions.

3.2.2. Parameters linked to the filling of the vessel

The number of pebbles and the mass of powder introduced into the vessel are characterized by the filling ratios J for the pebbles and f_c for the powder. They correspond to the ratio between the apparent volume occupied by the pebbles bed V_{pebbles} or by the powder bed V_{powder} and the total volume of the vessel V as described in equation (5).

$$J = \frac{V_{\text{pebbles}}}{V} \text{ and } f_c = \frac{V_{\text{powder}}}{V} \tag{5}$$

The flow function coefficients of the ground powder obtained for various pebbles filling ratio set to $J = 0.1$, 0.3 and 0.5, with a constant powder filling ratio set to $f_c = 3.3\%$ are shown by the hatched bars on Fig. 10. It clearly appears that the grinding process is highly affected by the pebbles filling ratio. An intermediate ratio of $J = 0.3$ seems to be the most efficient to grind the powders investigated as compared to the other pebbles filling ratio considered. However, the powder filling ratio, f_c, which characterizes the amount of powder within the vessel, also seems to be a critical parameter that defines the properties of the resulting ground powder. Indeed, it appears on Fig. 10, that the flow function coefficient obtained for the powder ground with $J = 0.3$ and $f_c = 9.9\%$, is twice higher than the one measured for the same powder ground with $f_c = 3.3\%$ and with the same pebbles filling ratio, J. This result can be explained by the fact that the particle fragmentation depends on the specific energy provided to the particles, as suggested by the energetic laws developed by Von Rittinger, Kick and Bond [25]. This means that the ratio between the number of pebbles and the amount of powder should also be considered. The powder level, classically denoted as U and defined by equation (6), can be used to describe such a ratio. A powder level equal to $U = 1$ means that the powder bed fills all the porosity, ε_g, between the pebbles and thus arises at the same level than the pebbles bed into the vessel before grinding.

$$U = \frac{V_{\text{powder}}}{\varepsilon_g \cdot V_{\text{pebbles}}} = \frac{f_c}{\varepsilon_g \cdot J} \tag{6}$$

The powder level corresponding to the grinding conditions represented by the hatched bars on Fig. 10 are given in the associated table. The variation of the powder flowability as a function of J can then be interpreted as representative of the effect of the powder level used instead of being related to the pebbles filling ratio only. Thus, another set of experiments was carried out, by varying the pebbles filling ratio while adjusting the amount of powder poured into the vessel in order to maintain a constant level of powder set to $U = 1$. The results, represented by the dotted bars on Fig. 10 seem to confirm that maintaining the same powder level in the vessel allows to obtain similar results in terms of flowability, even

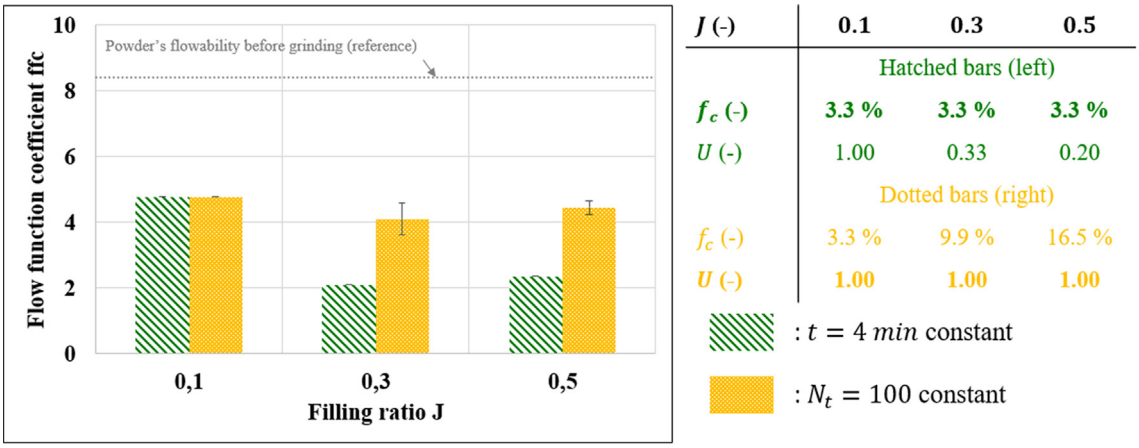

Fig. 10. Evolution of the flow function coefficient of ground powders according to the pebbles filling ratio J at constant powder filling ratio f_c (hatched bars, left) and constant level of powder U (dotted bars, right). All the grinding tests are performed in the same conditions with $\Omega = 25rpm$ and $t = 4min$.

if different pebbles and powder filling ratios are considered. However, we can notice that the flow function coefficient of the powder ground with a filling ratio of $J = 0.3$ and a level of powder of $U = 1.00$ appears slightly lower than the one obtained for $J = 0.1$ and $J = 0.5$ with the same powder level. Accordingly, an optimal pebbles filling condition for grinding is situated around $J = 0.3$ as suggested in previous experimental studies [3,26] and recently confirmed by discrete-element simulations [6].

4. Dimensional analysis

After investigating the most common grinding parameters in the 1 L vessel in section 3, a more precise analysis will then be developed in the following in order to provide scaling criteria for the ball mill process that could apply to larger vessels. The dimensional analysis will be carried out using the well-known Buckingham-Pi method [27].

4.1. Application of the Buckingham-Pi method

The Buckingham-Pi method consists in identifying all the variables of interest for a given system and organizing them into non-dimensional quantities that are believed to fully describe this system. When applied to process scale-up, this approach provides dimensionless groups that, when maintained constant, allows keeping a given property constant [14]. In particular, it is commonly used for guiding industrial manufacturers for replicating an industrial process at a laboratory or pilot scale or deducing the behavior of a process from results obtained at much smaller scale [12,13]. In the frame of the investigations reported in this paper, the Buckingham-Pi method is applied to the ball mill system in order to deduce the most significant dimensionless groups involved in the ball mill process whatever the size of the vessel used.

4.2. Definition of the system and identification of the variables of interest

In this section, the ball mill system will be described into details by identifying the physical variables that seem to be relevant for the ball milling process. All the variables identified are summarized in Table 3.

First, the grinding process takes place into a cylindrical vessel which can be characterized by its inner diameter D_i and its length L. The vessel is filled with cylindrical pebbles characterized by their diameter d_g and their height l_g. In this study, only the size d_g of the pebbles will be taken into account since all the pebbles used share the same aspect ratio of $\lambda_g = d_g/l_g = 1$. The porosity of the pebbles bed ε_g could not be measured directly by it will not be taken into account because it is not supposed to change with the dimensions of the mill, provided that any wall effect is negligible. Such an assumption seems reasonable considering the size of the pebbles as compared to the diameters of the vessels, however, one should keep this in mind when analyzing the results. Similarly, since all the vessels and pebbles are made of the same materials, the wall friction coefficient μ_w between the vessel and the pebbles and the density of the pebbles ρ_g will not be taken into account. The number of pebbles introduced within the vessel is characterized by the apparent volume of the pebbles bed V_{pebbles} when the vessel is at rest.

The vessel is rotating horizontally in the longitudinal axis with an angular velocity ω under the gravity acceleration g for a given grinding time t. The rotation of the vessel triggers the movements of the pebbles bed, which forms an average slope angle ϕ with the horizontal, as shown on Fig. 4 and on Fig. 5. At the powder bed surface, the pebbles are falling at an average speed of $v_g = \|\vec{v}_g\|$ as represented on Fig. 5.

Table 3
Physical variables of interested identified for the dimensional analysis of the ball milling process with their dimensions (M for mass, L for length and T for time).

Parameter	Notation	Usual units	Dimension
Vessel and pebbles properties			
Inner diameter of the vessel	D_i	mm	L
Length of the vessel	L	mm	L
Diameter of a pebble	d_g	mm	L
Powder properties			
Bulk density of the powder	ρ_p	g.cm^{-3}	M.L^{-3}
Initial properties of the particles	$\wp_i$	various	–
Final properties of the particles	$\wp_f$	various	–
Characteristic time of fragmentation	τ_0	s	T
Rotational parameters			
Angular velocity of the vessel	ω	rad.s^{-1}	T^{-1}
Average speed of a falling pebble	v_g	cm.s^{-1}	L.T^{-1}
Average slope angle	ϕ	°	ø
Grinding time	t	min	T
Filling parameters			
Apparent volume occupied by the pebbles	V_{pebbles}	ml	L^3
Mass of powder	m_p	g	M
Other parameters			
Gravity acceleration	g	m.s^{-2}	L.T^{-2}

Finally, the amount of powder is characterized by the mass of powder m_p poured into the vessel and by its bulk density ρ_p before grinding. A column vector $\wp$ will be used to describe the properties of the particles that may affect the flowability of the powders; this may include particle size distribution, specific surface area, surface roughness, surface energy and shape descriptors associated to the particles. Since those properties are likely to vary through the grinding process, the column vectors $\wp_i$ and $\wp_f$ will be used to describe the value of these parameters before and after grinding respectively. The rheology of a given powder is mostly controlled by the interaction between its constituting particles. The flowability of a ground powder is then expected to vary with the values contained in the $\wp$ vector. Moreover, in order to take into account the particles fragmentation, a tensile threshold stress, σ_0, which represents the internal cohesion of the particles and thus defines the minimum amount of energy required to break them, is considered. A characteristic fragmentation time, τ_0, can be obtained from σ_0 according to equation (7), which corresponds to the characteristic time between two successive fragmentation events. An analogous approach can be found in [23].

$$\tau_0 = \frac{1}{g}\sqrt{\frac{\sigma_0}{\rho_s}} \tag{7}$$

where ρ_s represents the true density of the powder. For this dimensional analysis, the characteristic fragmentation time τ_0 will be used instead of the tensile stress threshold σ_0.

4.3. Identification of the dimensionless groups

To summarize, a total of $\mathfrak{n} = 14$ physical parameters were identified. They are presented in Table 3 with the corresponding units and dimensions. According to this Table 3, all parameters can be expressed using only $\mathfrak{f} = 3$ elementary dimensions: mass, length and time. Then, the Vaschy-Buckingham theorem states that the whole system can be described from $\mathfrak{p} = \mathfrak{n} - \mathfrak{f} = 11$ dimensionless numbers, which can be identified by combining together the physical parameters of the system investigated. The system of variables $\{\rho_p, D_i, \omega\}$ was chosen as a basis to express all the other physical parameters. The dimensions of the variables expressed in the new basis are given in Table 4. Concerning the $\wp_i$ and $\wp_f$ vectors representing the initial and final properties of the powder, their dimension could not be precisely defined since it depends on the properties considered (particle sizes, specific surface area, surface energy...). Anyway, the dimensions of $\wp_i$ and $\wp_f$ are expected to be a combination of mass, length and time. The corresponding dimensionless numbers $\pi_{10} = f(\wp_i)$ and $\pi_{11} = f(\wp_f)$ will be addressed later in this section. The other dimensionless numbers are: $\pi_1 = L/D_i$, $\pi_2 = d_g/D_i$, $\pi_3 = \tau_0 \cdot \omega$, $\pi_4 = v_g/(D_i \cdot \omega)$, $\pi_5 = \phi$, $\pi_6 = t \cdot \omega$, $\pi_7 = V_{\text{pebbles}}/{D_i}^3$, $\pi_8 = m_p/\left(\rho_p \cdot {D_i}^3\right)$ and $\pi_9 = g/(D_i \cdot \omega^2)$.

The final dimensionless numbers can then be defined by combining the primary dimensionless numbers $\pi_{i=1:11}$ together. All the definitive dimensionless numbers obtained are then summarized and defined in Table 5. Among them, the aspect ratio of the vessel λ and the pebble-vessel ratio δ are linked to the geometrical configuration of the system investigated. The pebbles filling ratio J and the level of powder U, as defined previously in section 3.2.2, are both related to the vessel filling conditions.

The number of revolutions of the vessel N_t and the number of fragmentation events n_f are both related to the grinding time. Finally, the Froude number Fr, the velocity ratio v and the average slope angle of the bed ϕ are related to the vessel and pebbles movement. The relation linking those three parameters has already been investigated by a velocimetry analysis carried out in section 3.1. In particular, it appeared on Fig. 7 and Fig. 8 that setting the Froude number to a given value also defines the velocity ratio and the average slope angle. This is true, at least, in the range of vessel rotational speeds investigated in this study. Thus, those three parameters seem to be redundant and only the Froude number can be considered. The average slope angle of the pebbles bed, ϕ, and the velocity ratio, υ, can thus be removed from the list of dimensionless numbers presented in Table 5, which brings the actual number of independent non-dimensional groups to $\mathfrak{p} = 9$ instead of 11.

Concerning the initial and final properties of the powder bed characterized by the $\wp_i$ and $\wp_f$ vectors, they can be adimensionalized in the form of the granular Bond number Bo_g that corresponds to the ratio between interparticle cohesive forces and gravitational forces applied to the particles constituting the powder bed. The granular Bond number of a given powder can be computed from its constituting particle properties. It describes the resistance of the powder to gravitational flow due to cohesive behaviors of the particles [28]. In particular, this dimensionless granular Bond number was shown to correlate well with the macroscopic flowability of several powders, represented by the flow function coefficient [9]. Accordingly, the granular Bond numbers $\pi_{10} = Bo_{g,i}$ and $\pi_{11} = Bo_{g,f}$ can then be employed as dimensionless numbers to represent the flowability of the powders before and after grinding.

It should be noted that the dimensional analysis has been carried out specifically for the experimental setup used for the investigations reported in this paper. However, the friction coefficient between the wall and the pebbles μ_w, the pebble bed porosity ε_g, the pebble aspect ratio λ_g and their true density ρ_g should also be considered in addition to the other parameters described above in a more general case.

4.4. Scale-up criteria

According to the Vashy-Buckingham theorem, the whole system described in the section 4.2 can be fully defined by the 9 dimensionless numbers that are summarized in Table 5. In particular, that means that keeping 8 of these numbers constant while changing the dimensions of the equipment implies that the last one has to remain constant as well. This provides scale-up criteria for the ball milling process. Indeed, the flow properties of the ground powder, represented by its granular Bond number $Bo_{g,f}$ can be reproduced at any scale, providing that all the other dimensionless numbers are kept constant, as shown in equation (8). In this section, we will discuss the implications of keeping each dimensionless number constant for reproducing the ball mill process at any scale and targeting to keep $Bo_{g,f}$ constant.

$$Bo_{g,f} = F\left(\lambda; \delta; J; U; Bo_{g,i}; N_t; n_f; Fr\right) \tag{8}$$

Table 4
Physical variables expressed in the basis of the dimensions of.ρ_p, Di, ω

Variable	L	d_g	$\wp_i$	$\wp_f$	τ_0	v_g	ϕ	t	V_{pebbles}	m_p	g	ρ_p	D_i	ω
M	0	0	–	–	0	0	0	0	0	1	0	**1**	**0**	**0**
3 M + L	1	1	–	–	0	1	0	0	3	3	1	**0**	**1**	**0**
-T	0	0	–	–	−1	1	0	−1	0	0	2	**0**	**0**	**1**

Table 5
Dimensionless numbers obtained from the dimensional analysis of the ball mill process.

Dimensionless number	Notation and definition	Combination
Geometrical configuration		
Aspect ratio of the vessel	$\lambda = \frac{D_i}{L}$	$= {\pi_1}^{-1}$
Pebble to vessel ratio	$\delta = \frac{d_g}{D_i}$	$= \pi_2$
Filling conditions		
Pebble filling ratio (see equation (6))	$J = \frac{V_{pebbles}}{\frac{\pi}{4} {D_i}^2 L}$	$= \frac{4}{\pi} \cdot \pi_7 \cdot {\pi_1}^{-1}$
Level of powder	$U = \frac{m_p}{\rho_p \frac{\pi}{4} {D_i}^2 L}$	$= \frac{4}{\epsilon_g \pi} \cdot \pi_1 \cdot \pi_8$
Powder properties		
Granular Bond number before grinding	$Bo_{g,i} = \frac{F_{ip,i}}{W_p}$	$= \pi_{10}$
Granular Bond number after grinding	$Bo_{g,f} = \frac{F_{ip,f}}{W_p}$	$= \pi_{11}$
Rotation of the vessel		
Average slope angle	ϕ	$= \pi_5$
Velocity ratio	$v = \frac{2 v_g}{D_i \omega}$	$= 2\pi_4$
Froude number	$Fr = \frac{D_i \omega^2}{2g}$	$= \frac{1}{2} \cdot {\pi_9}^{-1}$
Grinding time		
Number of revolutions	$N_t = \omega t$	$= \pi_6$
Number of fragmentation events	$n_f = \frac{t}{\tau_0}$	$= \pi_6 \cdot {\pi_3}^{-1}$

First of all, the conservation of $Bo_{g,i}$ is almost trivial since it simply means that the same powder has to be used whatever the size of the mill, in order to obtain the same results in terms of final rheological properties. Then, the conservation of λ and δ provide geometric similitudes for the vessel and pebbles design. In particular, the conservation of δ implies that the size of the pebbles should be adjusted according to the size of the vessel. One can notice that with three vessel sizes (see Table 2) and only two pebbles sizes available (8x8 and 15x15 mm), the conservation of the ratio δ is not achieved systematically in this investigation. This issue will be discussed in section 5.1. The conservation of the J and U filling ratios can also be related to geometric similitudes since they tend to reproduce the same geometric configuration by adjusting the amounts of pebbles and powder to the vessel size. The importance of keeping the filling ratios constant has already been demonstrated experimentally for a single 1 L vessel in section 3.2.2. Moreover, keeping U and J constant implies that the powder filling ratio f_c remains also constant in virtue of equation (6). Thus, when the vessel's size changes, the conservation of $Bo_{g,i}$, λ, δ, J and U can be achieved relatively easily by using the same powder, dimensioning the vessel and the pebbles wisely and adjusting the number of pebbles and the mass of powder according to the considered configuration. The three remaining parameters are N_t, n_f and Fr, which are related to the vessel's rotational speed, ω, and to the grinding time, t. These parameters thus define which operational conditions should be chosen in order to get similar results in vessels of different scales, after dimensioning and filling them properly.

First, the vessel's rotational speed should be adjusted according to the Froude number, Fr, considered. The Froude number corresponds to the ratio between the centrifugal and gravitational forces acting on the pebbles located at the wall of the vessel. Thus, we can consider that the conservation of the Froude number leads to the respect of the dynamic similitudes through the scale up. The velocity ratio, v, and the average slope angle of the pebbles, ϕ, could also be considered since they were identified in the dimensional analysis. However, those two parameters were shown to be redundant with the Froude number for rolling rotational regimes in the velocimetry analysis carried out in section 3.1.

Finally, the number of revolution N_t is mainly related to the number of impacts caused by the pebbles that are projected at the bottom of the powder bed. From the powder point of view, the impact fragmentation appears to be a periodical phenomenon governed by the number of revolutions made by the vessel. On the other hand, the fragmentation number n_f is rather related to the collisions and frictions at a smaller scale between pebbles occurring anywhere within the pebbles bed, resulting in shearing fragmentation mechanisms. Thus, we can assume that N_t is mainly significant for fragmentation mechanism by impact while n_f is related to the fragmentation mechanism by shearing. Since the rotational speed of the vessel is already defined by the Froude number, the simultaneous conservation of N_t and n_f leads to a contradiction. Indeed, the grinding time, t, cannot be chosen according to N_t, which is related to the operational condition, and n_f, which only depends on the powder properties, at the same time. Thus, determining whether the scale-up of the ball mill is governed by N_t or n_f may provide meaningful information concerning the dominant mechanisms of fragmentation involved during ball milling process of a given powder. This matter is addressed in section 5.2.

5. Experimental results and discussion

The dimensional analysis carried out in section 4.1 provides dimensionless numbers that should be kept constant while changing the dimensions of the ball mill system, in order to obtain similar results in terms of powder flow. However, it is still unclear whether the grinding time should be adjusted to match a constant number of revolutions N_t or a constant number of fragmentations n_f. Before addressing this aspect in section 5.2, the effect of the pebble to vessel size ratio δ will be discussed in section 5.1.

5.1. Effects of the pebble to vessel size ratio

The experimental setup includes three sizes of vessels for only two sizes of pebbles. The pebble to vessel size ratios δ corresponding to each possible configuration are reported in Table 6. It appears that δ can be kept approximately constant between the 1 and 7 L vessels by using the 8x8 mm and 15x15 mm pebbles respectively. However, there is no configuration allowing us to keep δ constant between the 1 and 2 L vessels. In order to clarify the influence of the pebble to vessel ratio, the alumina powder has been ground in the 1 and 2 L vessels with both pebble geometries for various rotational speeds and grinding durations. The vessels rotational speeds were chosen in order to get constant Froude numbers, Fr, whatever the vessel used. Likewise, the grinding time was chosen in order to get an identical number of revolutions N_t. This implies that the fragmentation number, n_f, related to the characteristic fragmentation time, τ_0, was not exactly the same between both vessels. However, it can be assumed that they are quite close considering the similarity of the inner diameters for both vessels. For example, for a powder ground in the 1 L vessel with $Fr = 0.04$ and $N_t = 100$, the conservation of n_f in the 2 L vessel implies a grinding time of 4 min, while the grinding time was set to 4 min and 33 s in order to match $N_t = 100$. The flow function coefficients of the powder obtained in each grinding conditions were measured with the FT4® shear tester, as described in section 2.1.2. The results are shown on Fig. 11 where the incertitude intervals correspond to the standard deviations between two samples of

Table 6
Pebble to vessel ratios according to the pebble/vessel configuration. The number of pebbles needed to fill the vessel at $J = 0.3$ is given in parenthesis.

Vessel \ pebbles	8x8 mm	15x15 mm
1 L	$\delta = 6.9\%(N_g \approx 500)$	$\delta = 12.9\%(N_g \approx 75)$
2 L	$\delta = 5.5\%(N_g \approx 1000)$	$\delta = 10.3\%(N_g \approx 150)$
7 L	$\delta = 3.7\%(N_g \approx 3500)$	$\delta = 7.0\%(N_g \approx 530)$

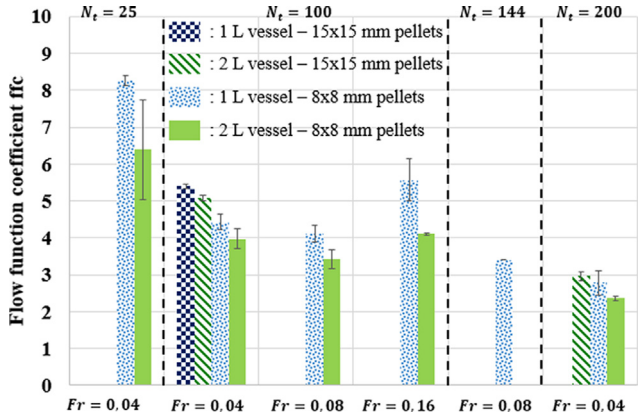

Fig. 11. Flow function coefficients of powder samples ground in various conditions using different vessels and pebbles.

the same ground powder that have been tested. It appears that the ground powder does not have the same flowability depending on the pebble/vessel configuration, despite the fact that the Froude number and the number of revolutions are kept constant and the number of fragmentations are very close. In particular, the flowability of the powder seems to decrease when the pebble to vessel ratio is smaller, even if the other non-dimensional groups are kept constant. This suggests that the efficiency of the grinding operation increases when using smaller pebbles. This result is consistent with previously reported experimental [29] and simulation [6] results. This can be explained by the fact that decreasing the pebbles size at fixed vessel filling ratios increases the total solid surface developed by the pebbles, promoting the shearing fragmentation mechanisms. Similarly, as far as smaller pebbles lead to a higher number of pebbles, N_g, it leads to a higher number of contacts between pebbles. As an example, the number of pebbles needed to fill the vessel at $J = 0.3$ in every pebble/vessel configurations is given in parenthesis in Table 6.

A focus on the grinding conditions defined by $Fr = 0.04$ and $N_t = 100$ is shown on Fig. 12, where all the possible pebble/vessel configurations for the 1, 2 and 7 L vessels were tested. Considering the 1 and 2 L vessels, it clearly appears that the flow function coefficient is lower when the pebble to vessel ratio decreases, meaning that the powder is more ground. However, this is no longer true when considering the powder ground in the 7 L vessel with the 15x15 mm pebbles. This configuration ensures a pebble to vessel ratio of $\delta = 7.0\%$, which is very close to the one obtained in the 1 L vessel using the 8x8 mm pebbles ($\delta = 6.9\%$), but gives a flow

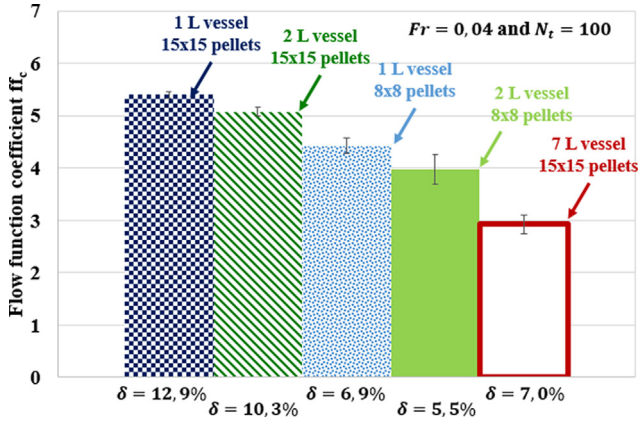

Fig. 12. Flow function coefficient of powder samples ground at $Fr = 0.04$ and $Nt = 100$ using various pebbles in the 1 L, 2 L and 7 L vessels.

function coefficient significantly smaller despite the conservation of Fr, N_t and δ parameters simultaneously. This probably comes from the fact that either the Froude number or the number of revolutions (or both) are not the most relevant quantities to keep constant through the scale up. This issue will be discussed in the next section 5.2.

5.2. Scaling up the ball milling process: Rotational speed and grinding time

We showed in the last section 5.1 that the conservation of the Froude number and the number of revolutions provide relatively good criteria for scaling up from the 1 L vessel to the 2 L one. However, this becomes less relevant when the dimensions of the vessel become more important, as for example with the 7 L vessel. Indeed, the conservation of these two dimensionless numbers failed to provide similar results as compared to the ones obtained in the 1 and 2 L vessels (as shown on Fig. 12). This suggests that other quantities, such as the wall velocity v_w for the rotational speed and the fragmentation number n_f for the grinding time, should be considered instead of the Froude number and the number of revolutions. Concerning the vessel rotational speed, the conservation of the wall velocity provides a kinetic similitude instead of the dynamic similitude associated to the conservation of the Froude number. To what concerns the grinding time, the conservation of the number of revolutions consists in adjusting the grinding time accordingly to the vessel's rotational speed in order to maintain the same number of full revolutions of the vessel at any scale. On the other hand, the conservation of the fragmentation number consists in maintaining the same amount of fragmentation events, which are characterized by a characteristic time τ_0. Since τ_0 only depends on the powder properties and do not depend on the grinding conditions, the conservation of the number of fragmentation simply leads to grinding for the same duration, whatever the size of the vessel.

In order to establish which ones of these quantities are the most relevant, a reference grinding experiment, denoted as $M^{[7]}$ was performed in the 7 L vessel, with the 15x15 pebbles, for a rotational speed of $\Omega = 25rpm$ and for a grinding time set to $t = 4min$. The corresponding Froude number, wall velocity, number of revolutions and fragmentation number are given in Table 7. Since the fragmentation characteristic time is not known, the number or fragmentation events is expressed in term of τ_0. Then, all the possible set of quantity conservations were tested in the 1 L vessel with the 8x8 mm pebbles. Such mock-up grindings are denoted as $m^{[1]}_{Fr-N_t}$, $m^{[1]}_{Fr-n_f}$, $m^{[1]}_{v_w-N_t}$ and $m^{[1]}_{v_w-n_f}$ according to the quantities chosen (see Table 7). By comparing the flowability obtained between the 1 and the 7 L vessels on Fig. 13, it appears that the grinding conditions leading to the most satisfactory results is $m^{[1]}_{Fr-n_f}$, where the Froude number and the fragmentation number are identical to those of $M^{[7]}$. All the other conditions, implying the conservation of the wall velocity or the number of revolutions failed to give similar results as compared to those obtained in the 7 L vessel. By the way, it is possible to check that all the other results presented on Fig. 13 are consistent. For example, the $m^{[1]}_{Fr-N_t}$ grinding test has the same Froude number than $M^{[7]}$ but a smaller fragmentation number, which leads to a higher flowability, interpreted as a less ground powder. On the other hand, the $m^{[1]}_{v_w-n_f}$ grinding test has the same fragmentation number but a higher Froude number than $M^{[7]}$ which leads to a more ground powder with a smaller flow function coefficient, as expected. Finally, the $m^{[1]}_{v_w-N_t}$ grinding test has about twice the Froude number of $M^{[7]}$ and half of its fragmentation number. However, the flow function coefficient is still higher than the

Table 7
Grinding conditions experimentally tested with the 1, 2 and 7 L vessels.

	vessel/pebble	$\Omega(rpm)$	t(s)	$Fr(-)$	$v_w(m \cdot s^{-1})$	$N_t(-)$	$n_f(-)$
$M^{[7]}$	7 L / 15x15 mm	25	240	**0.075**	**0.28**	**100**	**240 / τ_0**
$m^{[2]}_{Fr-n_f}$	2 L / 8x8 mm	30	240	**0.075**	0.23	120	**240 / τ_0**
$m^{[1]}_{Fr-N_t}$	1 L / 8x8 mm	34	176	**0.075**	0.21	**100**	167 / τ_0
$m^{[1]}_{Fr-n_f}$	1 L / 8x8 mm	34	240	**0.075**	0.21	136	**240 / τ_0**
$m^{[1]}_{v_w-N_t}$	1 L / 8x8 mm	46	130	0.137	**0.28**	**100**	130 / τ_0
$m^{[1]}_{v_w-n_f}$	1 L / 8x8 mm	46	240	0.137	**0.28**	276	**240 / τ_0**

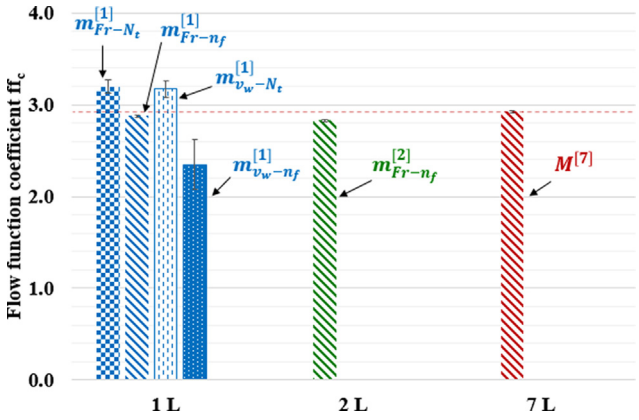

Fig. 13. Flow function coefficient of the powder samples ground in the conditions described in Table 7.

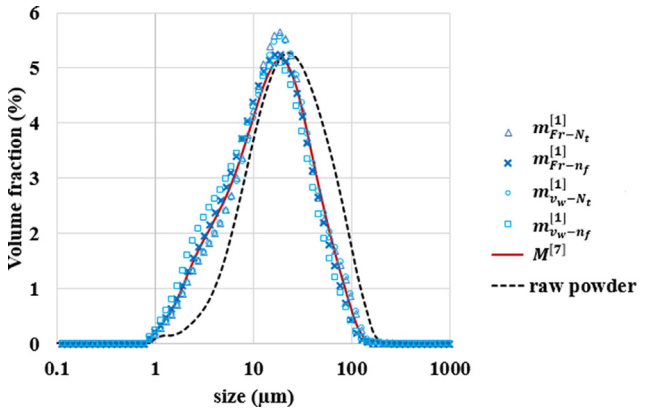

Fig. 14. Volume particle size distribution of the powder samples ground in the 1 L and the 7 L vessels in various conditions described in Table 7.

one obtained for $M^{[7]}$, suggesting that the fragmentation number has a larger impact on the flowability of the ground powders. These results show that the conservation of the Froude number and of the fragmentation number are the best criteria for scaling up the ball mill process in terms of flowability of the resulting ground powder. Since the flowability of powders is closely related to their particle size distribution [9], we can assume that these scaling criteria also ensures the conservation of the particle size after grinding. This point was verified by comparing the particle size distributions, obtained by LASER diffraction, for the mock-up grinding tests to that of the $M^{[7]}$ grinding test. The results are given on Fig. 14, where the raw powder, before grinding is represented in dotted line as a comparison. Once again, it appears that the $m^{[1]}_{Fr-n_f}$ grinding test is the one exhibiting the closest particle size distribution as compared to the powder ground in the 7 L vessel. The similarity of the volume particle size distributions obtained between the mock-up grinding tests (1 L vessel) and the reference grinding test (7 L vessel) can be assessed by comparing the corresponding Sauter mean diameters corresponding to the distributions. The total squared errors between the particle size distributions of the models and reference grindings has been calculated as well. The results, given in Table 8, shows that the $m^{[1]}_{Fr-n_f}$ grinding test almost perfectly reproduces the particle size distribution obtained in $M^{[7]}$. These results confirm that the Froude number and the fragmentation number are the most relevant dimensionless numbers that govern the grinding of powders in a ball mill.

In order to go further regarding these results, another grinding test, denoted $m^{[2]}_{Fr-n_f}$ was performed in the 2 L vessel, with the 8x8 mm pebbles. The rotational speed and the grinding time were adjusted so that Fr and the n_f are identical to those in the 7 L vessel. The measured flow function coefficient, shown on Fig. 13 is very similar to the one obtained in the 7 L vessel. The fact that the flow function coefficient of $m^{[2]}_{Fr-n_f}$ is slightly smaller than those of $m^{[1]}_{Fr-n_f}$ and $M^{[7]}$ can be explained by the smaller pebble to vessel size ratio in the test configuration used ($\delta = 5.5\%$) as compared to the 1 and 7 L configurations (respectively $\delta = 6.9\%$ and $\delta = 7.0\%$). As explained in section 5.1, a smaller pebble to vessel size ratio leads to a higher number of pebbles and thus a larger number of collisions for a constant vessel filling ratio J, which results in more grinding at a constant energy provided to the system.

Table 8
Sauter mean diameters corresponding to the particle size distributions of Fig. 14 and total squared error of the particle size distribution compared to the $M7$ grinding test.

	Sauter mean diameter $d_s(\mu m)$	Total squared error compared to the $M^{[7]}$ particle size distribution
$M^{[7]}$	8.8	0
$m^{[1]}_{Fr-N_t}$	9.3	2.072
$m^{[1]}_{Fr-n_f}$	8.5	1.049
$m^{[1]}_{v_w-N_t}$	9.4	1.666
$m^{[1]}_{v_w-n_f}$	7.7	3.754

As a conclusion to this section, we show that the rotational speed of the vessel should be adjusted to the vessel size in order to keep the Froude number constant. This implies that dynamic similitudes have to be taken into account rather than kinematic similitudes. Similarly, the grinding time should not vary whatever the vessel size in order to maintain the same fragmentation number. As discussed previously in section 4.4, the flowability of the ground powders would only be driven by the number of revolutions if the impact mechanisms were predominant among the particle fragmentation events. However, according to the results discussed in this section, the ball milling process seems to be mostly governed by the fragmentation number rather than the number of revolutions. Therefore, it can be speculated that grinding of alumina powder in a ball mill is mostly governed by shearing fragmentation mechanisms. However, it should be noted that the

grinding operation may be governed by the number of revolutions with coarser particles or at higher Froude numbers, corresponding to the cataracting regime, where the fragmentation of the particles by impact is more likely to occur.

6. Conclusion and perspectives

This paper provides an exhaustive dimensional analysis of a ball milling process of an alumina powder including a critical discussion about each parameters, based on experimental results. Scaling criteria are suggested in order to reproduce the flowability and the particle size distribution of the ground powders for various ball mill sizes. In particular, the importance of maintaining constant the pebble to vessel ratio δ, the filling ratios U and J, the Froude number Fr and the fragmentation number n_f, which basically leads to the conservation of the grinding time, were evidenced both theoretically and experimentally. In particular, this work shows that the size of the pebbles should be adjusted to the dimensions of the vessel in order to maintain the same specific surface area developed by the pebbles bed, which is a key parameter, related to the shearing fragmentation mechanisms. Other scaling criteria such as the vessel and pebbles aspect ratios λ and λ_g, the pebble bed porosity ε_g or the wall friction coefficient μ_w were also highlighted but could not be investigated experimentally.

The conservation of the Froude number, resulting in a dynamic similitude, was shown to reproduce effectively the motion of the pebbles within the pebbles bed. This was established by measuring the flowability and the particle size distribution of ground powder under various conditions, at different scales and by tracking the movement of the pebbles within the bed thanks to video recording. This also allowed us to evidence the transition between two motion regimes within the ball mill: a rolling regime for $Fr \leq 0.13$ in which the pebbles velocity is driven by the collisions with other pebbles and a cascading regime for $Fr \geq 0.13$ in which the pebbles velocity is proportional to the vessel wall velocity.

Finally, the number of particle fragmentation events was shown to govern the evolution of the flowability of the alumina ground powder rather than the number of revolutions of the vessel. This was interpreted as the result of the predominance of shearing fragmentation mechanisms over impact for alumina particles, in rolling and cascading motion regimes. It should be noted that the characteristic time of fragmentation τ_0 was assumed to be the same for each particle constituting the powder bed. However, one can expect that the mechanisms and the kinetics of fragmentation depend on the size of the particles involved. Therefore, it would be of great interest to investigate the mechanisms of fragmentation of the alumina particles according to the particle size distribution. This could be achieved by defining the characteristic time of fragmentation from the selection and breakage matrices commonly used for the population balance simulation of the grinding operations [30]. In particular, the selection function can be interpreted as a kinetic constant associated to each particle size class within the powder [25]. Therefore, a population dependent characteristic time of breakage could be defined by taking the inverse of the selection function. Such considerations should be further explored in future investigations.

The scaling criteria established in this study were shown to be consistent for extrapolating the results for vessels from 1 L to 7 L, which corresponds to sizes from the laboratory to the pilot scale. However, one can wonder if these principles could also be applied for extrapolations to larger scales. In a similar investigation, Mayer-Laigle [31,32] used the principle of similarities to establish scale-up laws for a powder mixing operation carried out in Turbula® mixers. The scaling criteria obtained allowed to get similar mixtures with vessels from 2 L to 17 L. However, significant differences were observed when applying these criteria to an industrial vessel of 50 L, suggesting that other mechanisms must be considered when extrapolating at larger scales. According to the authors, this could be due to the larger free surface available at the top of the powder bed that may induce more percolation in the industrial mixer. This means that the criteria obtained during our investigations should be considered with care when extrapolating to the industrial scale. This matter should be investigated in more details in further studies.

Declaration of Competing Interest

The authors declare that they have no known competing financial interests or personal relationships that could have appeared to influence the work reported in this paper.

References

[1] L.G. Austin, R.S.C. Rogers, Powder technology in industrial size reduction, Powder Technol. 42 (1) (1985) 91–109, https://doi.org/10.1016/0032-5910(85)80041-3.

[2] A.S. Erdem, Ş.L. Ergün, The effect of ball size on breakage rate parameter in a pilot scale ball mill, Miner. Eng. 22 (7) (2009) 660–664, https://doi.org/10.1016/j.mineng.2009.01.015.

[3] K. Shoji, L.G. Austin, F. Smaila, K. Brame, P.T. Luckie, Further studies of ball and powder filling effects in ball milling, Powder Technol. 31 (1) (1982) 121–126, https://doi.org/10.1016/0032-5910(82)80013-2.

[4] V.K. Gupta, Effect of size distribution of the particulate material on the specific breakage rate of particles in dry ball milling, Powder Technol. 305 (Jan. 2017) 714–722, https://doi.org/10.1016/j.powtec.2016.10.075.

[5] A. Alexander, T. Shinbrot, F.J. Muzzio, Scaling surface velocities in rotating cylinders as a function of vessel radius, rotation rate, and particle size, Powder Technol. 126 (2) (2002) 174–190, https://doi.org/10.1016/S0032-5910(02)00010-4.

[6] L. Orozco, D.-H. Nguyen, J.-Y. Delenne, P. Sornay, F. Radjai, Discrete-element simulations of comminution in rotating drums: Effects of grinding media, Powder Technol. 362 (2020) 157–167, https://doi.org/10.1016/j.powtec.2019.12.014.

[7] Y. Arai, Chemistry of Powder Production. Springer Netherlands, 1996. [Online]. Available: https://books.google.fr/books?id=6Bgew6-rNgwC

[8] J. Mellmann, The transverse motion of solids in rotating cylinders—forms of motion and transition behavior, Powder Technol. 118 (3) (Aug. 2001) 251–270, https://doi.org/10.1016/S0032-5910(00)00402-2.

[9] M. Giraud et al., "Investigation of a granular Bond number based rheological model for polydispersed particulate systems," Chem. Eng. Sci., p. 115971, 2020, doi: https://doi.org/10.1016/j.ces.2020.115971.

[10] A. Madian, M. Leturia, C. Ablitzer, P. Matheron, G. Bernard-Granger, K. Saleh, Impact of fine particles on the rheological properties of uranium dioxide powders, Nucl. Eng. Technol. 52 (8) (2020) 1714–1723, https://doi.org/10.1016/j.net.2020.01.012.

[11] H. Lu, X. Guo, Y. Liu, X. Gong, Effect of Particle Size on Flow Mode and Flow Characteristics of Pulverized Coal, KONA Powder Part. J. 32 (2015) 143–153, https://doi.org/10.14356/kona.2015002.

[12] A.S. Bongo Njeng, S. Vitu, M. Clausse, J.-L. Dirion, M. Debacq, Effect of lifter shape and operating parameters on the flow of materials in a pilot rotary kiln: Part II. Experimental hold-up and mean residence time modeling, Powder Technol. 269 (2015) 566–576, https://doi.org/10.1016/j.powtec.2014.05.070.

[13] E. Olmos, K. Loubiere, C. Martin, G. Delaplace, A. Marc, Critical agitation for microcarrier suspension in orbital shaken bioreactors: Experimental study and dimensional analysis, Chem. Eng. Sci. 122 (2015) 545–554, https://doi.org/10.1016/j.ces.2014.08.063.

[14] G. Delaplace, Modélisation en génie des procédés par analyse dimensionnelle : Méthode et exemples résolus. 2014.

[15] Y.L. Ding, R. Forster, J.P.K. Seville, D.J. Parker, Granular motion in rotating drums: bed turnover time and slumping–rolling transition, Powder Technol. 124 (1) (2002) 18–27, https://doi.org/10.1016/S0032-5910(01)00486-7.

[16] F. Pignatel, C. Asselin, L. Krieger, I.C. Christov, J.M. Ottino, R.M. Lueptow, Parameters and scalings for dry and immersed granular flowing layers in rotating tumblers, Am. Phys. Soc. 86 (1) (2012), https://doi.org/10.1103/PhysRevE.86.011304 011304.

[17] A.A. Boateng, P.V. Barr, Granular flow behaviour in the transverse plane of a partially filled rotating cylinder, J. Fluid Mech. 330 (1) (1997) 223–249, https://doi.org/10.1017/S0022112096003680.

[18] L. Orozco, J.-Y. Delenne, P. Sornay, F. Radjai, Rheology and scaling behavior of cascading granular flows in rotating drums, J. Rheol. 64 (2020) 915–931, https://doi.org/10.1122/1.5143023.

[19] K. Yamane, M. Nakagawa, S. A. Altobelli, T. Tanaka, and Y. Tsuji, "Steady particulate flows in a horizontal rotating cylinder," Physics of Fluids, vol. 10, no. 6, 1998, doi: 10.1063/1.869858.

[20] EFCE, Standard shear testing technique for particulate solids using the jenike shear cell, EFCE Working Party on the Mechanics of Particulate. Institution of

Chemical Engineers, 1989. [Online]. Available: https://books.google.fr/books?id=NB4Wunt4vo0C
[21] M. Leturia, M. Benali, S. Lagarde, I. Ronga, K. Saleh, Characterization of flow properties of cohesive powders: A comparative study of traditional and new testing methods, Powder Technol. 253 (2014) 406–423, https://doi.org/10.1016/j.powtec.2013.11.045.
[22] J. P. Seville, U. Tüzün, and R. Clift, Processing of Particulate Solids. Springer Netherlands, 2012. [Online]. Available: https://books.google.fr/books?id=oCnyCAAAQBAJ
[23] L. Orozco, J.-Y. Delene, P. Sornay, F. Radjai, Scaling behavior of particle breakage in granular flows inside rotating drums, Am. Phys. Soc. 101 (5) (2020), https://doi.org/10.1103/PhysRevE.101.052904 052904.
[24] M. Giraud et al., Predicting the flowability of powder mixtures from their single components properties through the multi-component population-dependent granular bond number; extension to ground powder mixtures, Powder Technol. 379 (2021) 26–37, https://doi.org/10.1016/j.powtec.2020.10.046.
[25] C. L. Prasher, Crushing and grinding process handbook. Wiley, 1987. [Online]. Available: https://books.google.fr/books?id=lNZTAAAAMAAJ
[26] E. Petrakis, E. Stamboliadis, K. Komnitsas, Identification of Optimal Mill Operating Parameters during Grinding of Quartz with the Use of Population Balance Modeling, KONA Powder Part. J. 34 (2017) 213–223, https://doi.org/10.14356/kona.2017007.
[27] E. Buckingham, On Physically Similar Systems; Illustrations of the Use of Dimensional Equations, Am. Phys. Soc. 4 (4) (1914) 345–376, https://doi.org/10.1103/PhysRev.4.345.
[28] M. Capece, K.R. Silva, D. Sunkara, J. Strong, P. Gao, On the relationship of inter-particle cohesiveness and bulk powder behavior: Flowability of pharmaceutical powders, Int. J. Pharm. 511 (1) (Sep. 2016) 178–189, https://doi.org/10.1016/j.ijpharm.2016.06.059.
[29] A. L. Mular, G. V. Jergensen, and S. of M. E. of AIME. M. P. Division, Design and installation of comminution circuits. Society of Mining Engineers of the American Institute of Mining, Metallurgical, and Petroleum Engineers, 1982. [Online]. Available: https://books.google.fr/books?id=yUPrAAAAMAAJ
[30] L.G. Austin, Introduction to the mathematical description of grinding as a rate process, Powder Technol. 5 (1) (1971) 1–17, https://doi.org/10.1016/0032-5910(71)80064-5.
[31] C. Mayer-Laigle, ‘‘Étude dynamique et effet du changement d’échelle pour plusieurs systèmes particulaires en mélangeur Turbula® : application à un mélange destiné à la fabrication de plaques composites,” Université de Toulouse, 2012. Accessed: Apr. 04, 2017. [Online]. Available: http://ethesis.inp-toulouse.fr/archive/00001926/01/laigle.pdf
[32] C. Mayer-Laigle, C. Gatumel, H. Berthiaux, Scale-up in Turbula® mixers based on the principle of similarities, Part. Sci. Technol. 38 (8) (Nov. 2020) 973–984, https://doi.org/10.1080/02726351.2019.1644689.